ON THE ANALYSIS OF HIDDEN OSCILLATIONS AND MULTISTABILITY IN THE KELDYSH MODEL OF FLUTTER SUPPRESSION

Nikolay V. Kuznetsov
Department of Applied Cybernetics,
St. Petersburg State University,
7-9 Universitetskaya nab.,
St. Petersburg, 199034, Russia
Institute of Problems
in Mechanical Engineering of RAS,
61 Bolshoy prospekt V.O.,
St. Petersburg, 199178, Russia
nkuznetsov239@mail.ru

Ruslan N. Mokaev, Timur N. Mokaev
Department of Applied Cybernetics,
St. Petersburg State University,
7-9 Universitetskaya nab.,
St. Petersburg, 199034, Russia
r.mokaev@spbu.ru, t.mokaev@spbu.ru

Boris R. Andrievsky
Department of Applied Cybernetics,
St. Petersburg State University,
7-9 Universitetskaya nab.,
St. Petersburg, 199034, Russia
Institute of Problems
in Mechanical Engineering of RAS,
61 Bolshoy prospekt V.O.,
St. Petersburg, 199178, Russia
b.andrievsky@spbu.ru

Elena V. Kudryashova, Olga A. Kuznetsova
Department of Applied Cybernetics,
St. Petersburg State University,
7-9 Universitetskaya nab.,
St. Petersburg, 199034, Russia
e.kudryashova@spbu.ru, o_a_kuznetsova@mail.ru

Article history:
Received 03.06.2026, Accepted 19.06.2026

Abstract

This paper studies multistability and hidden oscillations in a four-dimensional Keldysh model of flutter suppression. The model is written in the Lurie form and is considered with discontinuous damper characteristics interpreted in the sense of Filippov. We analyze the stationary set, the sliding manifold, and the corresponding reduced sliding dynamics. To detect undesired periodic solutions, we apply the locus of a perturbed relay system (LPRS) method and extend it to a discontinuous piecewise-linear approximation of the original Keldysh nonlinearity. It allows to reveal symmetric and asymmetric stable periodic solutions, including periodic solutions with complicated switching configurations. Numerical continuation from the discontinuous piecewise-linear characteristic to the original discontinuous characteristic with a quadratic term detects five stable periodic solutions, four of which are hidden with respect to the rest segment. These results show that the four-dimensional Keldysh model has rich and complex nonsmooth dynamics and provide a constructive framework for estimating the boundary of global stability in discontinuous aircraft control systems.

Key words

the Keldysh model, flutter suppression, multistability, hidden oscillations, LPRS, numerical continuation method

1 Introduction

In the work [Keldysh, 1944], Keldysh proposed a nonlinear model for flutter suppression using a hydraulic damper. The damper characteristic contains viscous and dry-friction components and is therefore essentially nonlinear and discontinuous. As a result, the analysis of the Keldysh model requires considering differential equations with discontinuous right-hand sides [Filippov, 1988; Gelig et al., 1978; Utkin et al., 2017; Boiko, 2008; Dolgopolik and Fradkov, 2017; Leonov et al., 2017]. From the viewpoint of modern nonlinear dynamics, this model is closely related to multistability and hidden oscillations, which leads to the problem of localizing coexisting attractors [Leonov and Kuznetsov, 2018a; Leonov and Kuznetsov, 2018b; Kuznetsov, 2020; Dudkowski et al., 2016; Leonov and Kuznetsov, 2013; Kolinichenko, 2024].

In [Boiko et al., 2026], the two-dimensional Keldysh model with a piecewise-linear characteristic was studied. This characteristic preserves the key qualitative features of the Keldysh dynamics and provides a discontinuous piecewise-linear approximation suitable for analytical and analytical–numerical frequency-domain analysis (see e.g. [Gelig et al., 1978; Leonov et al., 1996; Boiko, 2008; Leonov et al., 2017; Elsakov et al., 2024]. In that work, the describing-function method, Poincare map analysis, and the locus of a perturbed relay system (LPRS) [Boiko, 2008] were used to analyze periodic solutions and their orbital stability.

The aim of the present paper is to extend the above approach to the four-dimensional Keldysh model. The paper is organized as follows. Section 2 introduces the four-dimensional Keldysh model in the Lurie form and discusses its Filippov interpretation, including the rest segment and the sliding surface. Section 3 develops an LPRS-based approach for detecting periodic solutions and presents numerical experiments for the relay and discontinuous piecewise-linear characteristics, and original discontinuous characteristic with a quadratic term. The concluding section summarizes the results of the study and discusses the limitations of the proposed procedures.

2 Keldysh model of flutter suppression

The Keldysh system can be written in the Lurie form as follows [Leonov and Kuznetsov, 2018a]:

$$\dot{x} = A\,x + B\,\varphi(C^{\intercal}x), \tag{1}$$

where $x = (x_1, x_2, x_3, x_4)^{\intercal}$ is the state vector, $A = Q^{-1}\widetilde{A}$, $B = Q^{-1}\widetilde{B}$,

$$\widetilde{A} = \begin{pmatrix} 0 & 1 & 0 & 0 \\ -a_{11} & -b_{11} & -a_{12} & -b_{12} \\ 0 & 0 & 0 & 1 \\ -a_{21} & -b_{21} & -a_{22} & -(b_{22}+\lambda) \end{pmatrix}, \tag{2}$$

$$Q = \begin{pmatrix} 1 & 0 & 0 & 0 \\ 0 & c_{11} & 0 & c_{12} \\ 0 & 0 & 1 & 0 \\ 0 & c_{21} & 0 & c_{22} \end{pmatrix}, \quad \widetilde{B} = \begin{pmatrix} 0 \\ 0 \\ 0 \\ -1 \end{pmatrix}, \quad C = \begin{pmatrix} 0 \\ 0 \\ 0 \\ 1 \end{pmatrix}, \tag{3}$$

where λ, a_{ij}, b_{ij}, and c_{ij}, $i, j \in \{1, 2\}$, are real physical parameters of the original Keldysh model so that $\det Q \neq 0$. The scalar nonlinear characteristic $\varphi(\sigma)$ (original discontinuous characteristic with a quadratic term) is defined as follows:

$$\varphi(\sigma) = \left(\Phi + \kappa\sigma^2\right)\operatorname{sign}(\sigma). \tag{4}$$

The scalar transfer function of the linear part from the nonlinear feedback input to the scalar variable $C^{\intercal}x$ is given by

$$W(s) = \frac{N(s)}{D(s)},$$

where

$$\begin{aligned} N(s) &= s(c_{11}s^2 + b_{11}s + a_{11}), \\ D(s) &= (c_{22}s^2 + (b_{22}+\lambda)s + a_{22})(c_{11}s^2 + b_{11}s + a_{11}) - \\ &\quad - (c_{21}s^2 + b_{21}s + a_{21})(c_{12}s^2 + b_{12}s + a_{12}). \end{aligned}$$

Following [Leonov and Mokaev, 2017; Leonov and Kuznetsov, 2018a; Mokaev, 2019], we fix the coefficients of the linear part of the Keldysh system by setting

$$\begin{aligned} &a_{11} = a_{22} = b_{22} = c_{11} = c_{22} = 0, \\ &a_{21} = m_1^2 + \beta^2, \; a_{12} = m_2^2 + \beta^2, \\ &b_{11} = -1, \; b_{12} = b_{21} = 2\beta, \; c_{12} = c_{21} = 1. \end{aligned}$$

With this choice, the corresponding matrices in the Lurie form (1) of the Keldysh system are

$$A = \begin{pmatrix} 0 & 1 & 0 & 0 \\ -(m_1^2+\beta^2) & -2\beta & 0 & -\lambda \\ 0 & 0 & 0 & 1 \\ 0 & 1 & -(m_2^2+\beta^2) & -2\beta \end{pmatrix},$$

$$B = \begin{pmatrix} 0 \\ -1 \\ 0 \\ 0 \end{pmatrix}, \qquad C = \begin{pmatrix} 0 \\ 0 \\ 0 \\ 1 \end{pmatrix}. \tag{5}$$

Following [Boiko et al., 2026], we consider two piecewise-linear approximations of φ:

$$\varphi_{\mathrm{relay}}(\sigma) = \Phi\operatorname{sign}(\sigma), \tag{6}$$

$$\varphi_{\mathrm{pwl}}(\sigma) = \Phi\operatorname{sign}(\sigma) + \psi(\sigma), \tag{7}$$

$$\psi(\sigma) = \begin{cases} 0, & |\sigma| \le \delta, \\ \hat{\kappa}\big(\sigma - \delta\operatorname{sign}(\sigma)\big), & |\sigma| > \delta, \end{cases}$$

$$\delta = \frac{1}{\sqrt{\kappa}}, \qquad \hat{\kappa} = 4\sqrt{\kappa}.$$

The nonlinearity (6) corresponds to the special relay case, while nonlinearity (7) represents a discontinuous piecewise-linear characteristic that can be decomposed into the sum of a relay part and a dead-zone part (see Fig. 1). These approximations provide a convenient framework [Boiko et al.,

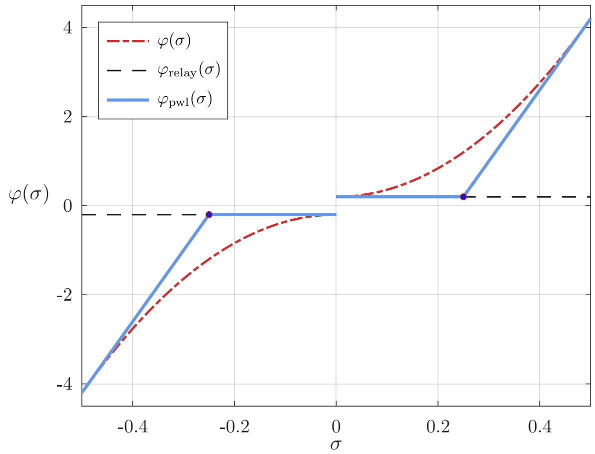

Figure 1. Three nonlinear characteristics of the damper in the Keldysh system.

2026] for studying periodic solutions by analytical and analytical–numerical techniques, including the describing-function and LPRS methods, as well as numerical continuation with respect to the parameters of the nonlinear characteristic.

Since the nonlinearities (4), (6), and (7) introduced above are discontinuous characteristics with a jump discontinuity only at $\sigma = 0$ (see Fig. 1), the corresponding systems are treated as differential inclusions, with solutions understood in the sense of Filippov [Filippov, 1988]. Namely, the value of each nonlinearity (4), (6), and (7) at the discontinuity is replaced by its set-valued regularization

$$\widehat{\phi}_\star(0) = [-\Phi, \Phi], \qquad \widehat{\phi}_\star(\sigma) = \{\phi_\star(\sigma)\}, \quad \sigma \neq 0. \tag{8}$$

Thus, the four-dimensional Keldysh system is written in the Lurie form as the differential inclusion

$$\dot{x} \in A\,x + B\,\widehat{\phi}_\star(C^\intercal x), \tag{9}$$

where $x \in \mathbb{R}^4$, $A \in \mathbb{R}^{4\times4}$, and $B, C \in \mathbb{R}^4$ are defined in (5). Since the Filippov interpretation makes the nonlinear characteristic set-valued on the discontinuity surface $\Sigma = \{x \in \mathbb{R}^4 \mid \sigma = C^\intercal x = x_4 = 0\}$, the subsequent analysis must also address the rest segment, the sliding surface, and the associated switching behavior.

2.1 Analysis of stationary and sliding set and sliding dynamics

Following [Gelig et al., 1978] (see also [Kiseleva and Kuznetsov, 2015]), let us analyze stationary points, sliding manifolds, and sliding regimes in the Keldysh system (9).

We first show that stationary points x_{eq} can occur only on the discontinuity surface Σ, i.e. when $C^\intercal x_{\text{eq}} = 0$. Since the matrix A in (5) is nonsingular, the stationary points x_{eq} of (9) are solutions of the following inclusion

$$x_{\text{eq}} \in -A^{-1}B\,\widehat{\phi}_\star(C^\intercal x_{\text{eq}}). \tag{10}$$

If $x_{\text{eq}} \notin \Sigma$, i.e. $C^\intercal x_{\text{eq}} \neq 0$, then the argument of the nonlinearity is different from zero and the inclusion (10) reduces to the equality

$$x_{\text{eq}} = -A^{-1}B\,\phi_\star(C^\intercal x_{\text{eq}}). \tag{11}$$

For the matrices A, B from (5), direct calculation gives

$$x_{\text{eq}} = \begin{pmatrix} -\dfrac{\phi_\star(C^\intercal x_{\text{eq}})}{m_1^2+\beta^2} \\ 0 \\ 0 \\ 0 \end{pmatrix}.$$

Its fourth component is necessarily zero: $C^\intercal x_{\text{eq}} = x_{\text{eq},4} = 0$, which contradicts the assumption $C^\intercal x_{\text{eq}} \neq 0$.

Thus, the stationary set $\mathcal{E}$ of the system (9), i.e. a set of all x_{eq}, belongs to the discontinuity surface Σ, and is embedded in the sliding manifold $\Sigma_{\text{sl}} \subset \Sigma$.

The sliding dynamics of system (9) on Σ_{sl} is defined as follows:

$$C^\intercal \dot{x} = 0 \in C^\intercal A x + C^\intercal B \widehat{\phi}_\star(0). \tag{12}$$

Using the matrices A, B, C from (5), we obtain $C^\intercal B = 0$, which implies for (12) the following

$$0 = C^\intercal A x. \tag{13}$$

Differentiating equation (13) with respect to system (9), we get the following condition

$$0 = C^\intercal A\dot{x} \in C^\intercal A^2 x + C^\intercal AB\,\widehat{\phi}_\star(0),\ \ x \in \Sigma_{\text{sl}}, \tag{14}$$

where $C^\intercal AB = -1 \neq 0$. Thus, from (8), (9), (13) and (14), the sliding manifold Σ_{sl} is given by

$$\begin{aligned} &C^\intercal x = 0, \quad C^\intercal A x = 0, \\ &\qquad -C^\intercal A\Phi B \geq C^\intercal A^2\,x \geq C^\intercal A\Phi B. \end{aligned} \tag{15}$$

Expression (15) can be rewritten in the following equivalent form:

$$\begin{aligned} \Sigma_{\text{sl}} = \Big\{ &(x_1, x_2, x_3, x_4) \in \mathbb{R}^4 : \\ &x_4 = 0,\ x_2 = (m_2^2+\beta^2)x_3,\ |q(x_1, x_3)| \leq \Phi \Big\}, \end{aligned} \tag{16}$$

where $q(x_1, x_3) = (m_1^2+\beta^2)x_1 + 2\beta(m_2^2+\beta^2)x_3$.

By substituting the expressions for x_2, x_3, and x_4 from (16) into (9), the sliding dynamics on $\Sigma_{\rm sl}$ is written as follows:

$$\dot{x}_1 = (m_2^2+\beta^2)x_3, \dot{x}_3 = 0, |q(x_1,x_3)| \le \Phi. \quad (17)$$

This reduced dynamics is valid as long as the trajectory remains on the sliding manifold, that is, as long as

$$\big|q(x_1(t),x_3(t))\big| \le \Phi.$$

At points where the sliding inequalities in (15) are strict, i.e. $|q(x_1,x_3)| < \Phi$, the vector fields of system (9) on the two sides of the discontinuity surface Σ are directed toward the sliding manifold $\Sigma_{\rm sl}$. Thus, for an initial point

$$\big(x_1(0),(m_2^2+\beta^2)x_3(0),x_3(0),0\big) \in \Sigma_{\rm sl},$$

the sliding motion on $\Sigma_{\rm sl}$ is defined uniquely as the solution of (17), namely,

$$x_3(t) \equiv x_3(0), \quad x_2(t) \equiv (m_2^2+\beta^2)x_3(0),$$
$$x_1(t) = x_1(0) + (m_2^2+\beta^2)x_3(0)t, \quad (18)$$

while the above condition for remaining on the sliding manifold is satisfied.

From (17), we obtain an explicit formula for the stationary set $\mathcal{E}$:

$$\mathcal{E} = \left\{(x_1,0,0,0) \in \mathbb{R}^4 : |x_1| \le \frac{\Phi}{m_1^2+\beta^2}\right\}. \quad (19)$$

3 LPRS-Based Search for Periodic Solutions

3.1 The LPRS method for relay systems

We use the LPRS method, developed for relay feedback systems [Boiko, 2008; Akimova et al., 2021], to detect symmetric and asymmetric periodic solutions with two relay switchings per period in the Keldysh system (9) with the relay characteristic (6).

Such a periodic solution is represented by two motion segments within the period $T > 0$: the first segment has duration μT, and the second one has duration $(1-\mu)T$, where $\mu \in (0,1/2]$. The symmetric case corresponds to $\mu = 1/2$, whereas asymmetric oscillations correspond to $\mu < 1/2$. Both cases are found by solving the following system for T and μ:

$$\begin{cases} C^{\mathsf T}x^{(1)}(T,\mu) = 0, \\ C^{\mathsf T}x^{(2)}(T,\mu) = 0, \end{cases} \quad (20)$$

where the state vectors at the switching instants are given by

$$x^{(1)} = (I-e^{AT})^{-1}A^{-1}\left(e^{AT} - 2e^{A(1-\mu)T} + I\right)B\Phi,$$
$$x^{(2)} = (I-e^{AT})^{-1}A^{-1}\left(-e^{AT} + 2e^{A\mu T} - I\right)B\Phi.$$

The obtained solutions are consistent with the assumed two-switching structure provided that no additional relay switchings occur within the period:

$$\sigma(t) > 0 \;\forall t \in (0,\mu T), \;\; \sigma(t) < 0 \;\forall t \in (\mu T, T). \quad (21)$$

3.2 LPRS-based extension to the characteristic

If a periodic solution of the relay system satisfies

$$|\sigma(t)| < \delta \quad \text{for all } t,$$

then the additional piecewise-linear term $\psi(\sigma)$ in (7) vanishes along this trajectory. Hence, the piecewise-linear characteristic (7) coincides with the relay characteristic (6) on this solution, and the relay LPRS equations remain applicable. Periodic motions that leave the strip $|\sigma| < \delta$ require an additional segment decomposition.

We now describe a procedure for localizing symmetric periodic solutions of the system (9) with the piecewise-linear nonlinearity (7) that leave the strip $|\sigma| < \delta$. In this case, the periodic solution consists of successive time segments. On each segment, the piecewise-linear characteristic either coincides with the relay characteristic or includes the additional piecewise-linear term $\psi(\sigma)$. Thus, the periodic solution is determined by matching the corresponding affine motions and imposing the threshold conditions at the boundaries of the strip. A similar procedure can be readily extended to locate asymmetric periodic solutions.

Let T be the period of a symmetric oscillation, and let $\rho = x(0) \in \mathbb{R}^4$ denote the state at the instant when the relay switches from $-\Phi$ to $+\Phi$. Consider the case in which, during the positive half-period, the trajectory first evolves inside the strip, then crosses the upper threshold $\sigma = \delta$, and finally returns to the strip before the next relay switching. Let $\theta_1, \theta_2, \theta_3 > 0$ be the lengths of these three successive time segments, so that

$$\theta_1 + \theta_2 + \theta_3 = \frac{T}{2}, \quad (22)$$

and denote:

$$\rho = x(0), \quad \eta = x(\theta_1),$$
$$\chi = x(\theta_1+\theta_2), \nu = x\left(\frac{T}{2}\right). \quad (23)$$

On the first segment, $0 \le C^{\mathsf T}x \le \delta$, the term $\psi(\sigma)$ vanishes, and the piecewise-linear characteristic reduces to the relay characteristic. Hence

$$\eta = e^{A\theta_1}\rho + A^{-1}\big(e^{A\theta_1} - I\big)B\,\Phi. \quad (24)$$

On the second segment, $C^{\mathsf T}x > \delta$, the additional piecewise-linear term becomes active, and the dynamics is affine with the modified matrix

$$A_1 = A + \hat{\kappa}\,BC^{\mathsf T}. \quad (25)$$

Therefore,

$$\chi = e^{A_1\theta_2}\eta + A_1^{-1}\big(e^{A_1\theta_2} - I\big)B\,(\Phi - \hat{\kappa}\delta). \qquad (26)$$

On the third segment, the trajectory returns to the strip $C^\intercal x \le \delta$, so that $\psi(\sigma) = 0$ again. By symmetry,

$$\begin{aligned}-\rho = \nu &= e^{A\theta_3}\chi + A^{-1}\big(e^{A\theta_3} - I\big)B\,\Phi = \\ &= e^{A\theta_3}\Big[e^{A_1\theta_2}e^{A\theta_1}\rho + e^{A_1\theta_2}A^{-1}\big(e^{A\theta_1} - I\big)B\,\Phi + \\ &\quad + A_1^{-1}\big(e^{A_1\theta_2} - I\big)B\,(\Phi - \hat{\kappa}\delta)\Big] + \\ &\quad + A^{-1}\big(e^{A\theta_3} - I\big)B\,\Phi.\end{aligned} \qquad (27)$$

Consequently, for each prescribed period T, symmetric periodic solutions of this type are localized by solving the algebraic system obtained from the threshold conditions

$$C^\intercal\eta = \delta, \qquad C^\intercal\chi = \delta, \qquad (28)$$

together with

$$\theta_3 = \frac{T}{2} - \theta_1 - \theta_2. \qquad (29)$$

Here η and χ are defined by (24) and (26), while the initial state ρ is determined from the symmetry condition (27). The numerical search can be formulated in terms of the segment lengths $\theta_1, \theta_2, \theta_3$, with the corresponding points ρ, η, and χ reconstructed from the linear transition formulas.

The resulting procedure for detecting periodic solutions in the Keldysh system with nonlinearity (7) can be organized as follows.

1. At the first stage, periodic solutions with two relay switchings per period are identified using the LPRS method applied to the system with the relay characteristic (6). The resulting solutions are then tested for the strip condition $|C^\intercal x| < \delta$. If this condition is satisfied over the whole period, the corresponding periodic solution is a periodic solution of the system with the piecewise-linear nonlinearity (7).
2. At the second stage, periodic solutions that are not entirely contained in the strip $|C^\intercal x| < \delta$ are localized by solving the finite-dimensional algebraic system derived from the segment-matching conditions. For a prescribed period T, or equivalently a prescribed frequency ω, solving the system of equations (27)–(29) determines the segment lengths and the corresponding initial state of the possible symmetric periodic solution. Then, each candidate is verified to ensure that there are no additional relay switchings or extra crossings of the thresholds $|C^\intercal x| = \delta$.

Table 1. Periodic solutions with two relay switchings per period detected by the LPRS method for the Keldysh system with relay nonlinearity.

Solution type	Initial state $x(0)$
Symmetric	0.05354250592466
	−0.5550749738252
	−1.697777714459
	0.0
Asymmetric	±1.511908966671
	∓0.9849357950153
	∓3.416190275531
	0.0

3. After the periodic solutions have been identified and verified, their orbital stability is determined from the spectrum of the monodromy matrix (see [Boiko et al., 2026]).

Thus, the proposed procedure extends the LPRS-based search to periodic solutions with two relay switchings per period whose trajectories may leave the strip $|C^\intercal x| < \delta$.

4 Analysis of the Four-Dimensional Keldysh System

To illustrate the proposed procedures, we consider a representative parameter set close to those used in previous studies of discontinuous Keldysh models [Leonov et al., 2017; Mokaev, 2019]:

$$\begin{aligned}m_1 = 0.9, \qquad m_2 = 1.1, \qquad \beta = 0.01, \\ \lambda = 0.01, \qquad \Phi = 0.2.\end{aligned} \qquad (30)$$

We consider successively the relay characteristic (6), the discontinuous piecewise-linear characteristic (7), and the original discontinuous characteristic with a quadratic term (4).

4.1 Relay characteristic

For the relay characteristic (6), the LPRS method was used to detect periodic motions with two relay switchings per period. For the chosen parameter values, the method gave one symmetric periodic solution with $T_{\text{sym}} = 11.90893183$ and $\mu = 1/2$, and two asymmetric periodic solutions with $T_{\text{asym}} = 9.32842724$ and $\mu = 0.348145509$. These two-switching solutions are shown in Fig. 2, and the corresponding initial data are given in Table 1.

A numerical search from randomly chosen initial data revealed the existence of three additional stable periodic solutions with a larger number of relay switchings per period. These solutions were not detected by the preceding LPRS-based procedure, since this procedure was designed for motions with two relay switchings per period; see Fig. 2 and Table 2.

We also note that, due to the Filippov interpretation, trajectories involving sliding segments on the

Table 2. Initial data for stable periodic solutions of the Keldysh system with the relay nonlinearity. In the rows containing the symbols $\pm$ and $\mp$, the signs are taken consistently.

Solution type	relay switchings	Initial state $x(0)$
Asymmetric	4	± 2.569661900009 ∓ 3.086739763650 ∓ 12.89457147432 0.0
Symmetric	6	3.334741174484 -1.476050606056 -5.280832913659 0.0

switching surface $C^\top x = 0$ could have been observed in direct numerical simulations; see the sliding set (16) and the reduced sliding dynamics (17). Such regimes were not included in the LPRS-based algebraic search, and no stable periodic motions with sliding segments were found in the simulations from randomly chosen initial data.

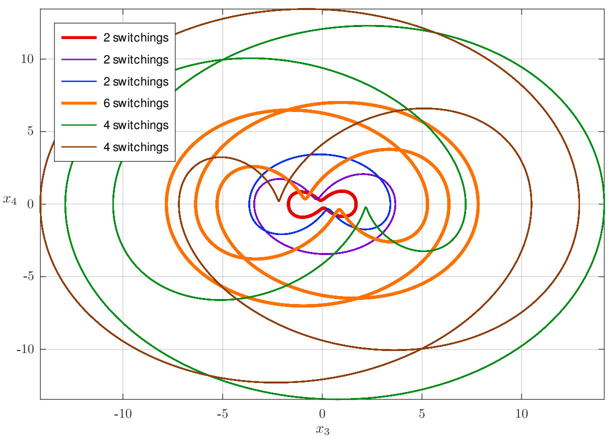

Figure 2. Periodic solutions of the Keldysh system with the relay nonlinearity. Thin curves correspond to asymmetric solutions, while thick curves correspond to symmetric solutions.

4.2 Modified discontinuous piecewise-linear characteristic

Among the relay periodic solutions found in the previous subsection, the symmetric one remains inside the strip $|C^\top x| < \delta$. Therefore, $\psi(\sigma)$ vanishes along this trajectory, and this solution is also obtained from the relay LPRS equations used at the first step of the procedure.

To trace the periodic regimes from the relay characteristic (6) to the piecewise-linear characteristic (7), points chosen on the localized periodic trajectories were used as initial conditions in a numerical continuation procedure [Dudkowski et al., 2016].

Table 3. Initial data for stable periodic solutions of the Keldysh system with discontinuous piecewise-linear characteristic.

No.	x_1	x_2	x_3	x_4
1	1.00956206	−2.71285688	−2.98187826	0.0
2	−1.66148401	−2.64796816	−2.97215912	0.0
3	0.01054611	−0.11096416	−0.33809656	0.0
4	−0.60941046	−3.64270022	−4.03018229	0.0
5	−0.09866127	−1.34918229	−1.62066720	0.0

This procedure traced the symmetric periodic solution to the system with the piecewise-linear nonlinearity.

The second step of the LPRS-based numerical procedure was then applied to solutions leaving the strip $|C^\top x| < \delta$. It revealed two asymmetric periodic solutions for which the additional piecewise-linear term becomes active.

In addition, a numerical search from randomly chosen initial data revealed two stable periodic regimes; see Figs. 3. The corresponding initial data are given in Table 3.

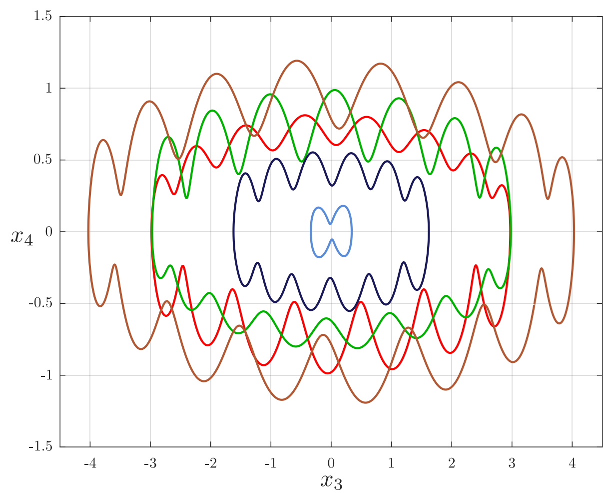

Figure 3. Periodic solutions of the Keldysh system with the discontinuous piecewise-linear characteristic.

4.3 Original Keldysh characteristic

Finally, points chosen from the periodic solutions detected for the modified nonlinearity (7) were used as initial conditions in a numerical continuation procedure from the modified characteristic to the original Keldysh nonlinearity (4). This procedure led to the detection of five periodic solutions of the original Keldysh system; see Fig. 4. The corresponding initial data are given in Table 4.

For the original Keldysh system, one of the five detected periodic solutions is self-excited, since it was visualized from a neighborhood of the unstable

Table 4. Points on the discontinuity surface $x_4 = 0$ for periodic solutions of the Keldysh system with the original discontinuous characteristic with a quadratic term.

No.	x_1	x_2	x_3	x_4
1	−0.37547844	−1.93657394	−2.27361056	0.0
2	−0.45965784	−2.55141934	−2.89380696	0.0
3	0.08295752	−0.05910113	−0.10442597	0.0
4	−0.55532966	−3.22277138	−3.55805171	0.0
5	−0.27781422	−0.89419971	−1.17066579	0.0

stationary set, whereas the remaining four are hidden oscillations [Leonov and Kuznetsov, 2013; Dudkowski et al., 2016] detected by continuation and from specially chosen initial data.

Furthermore, smoothing the discontinuous characteristic (4) by replacing $\operatorname{sign}(\sigma)$ with $\tanh(N\sigma)$, $N = 200$, leads to a smooth Lurie-type system with a unique locally asymptotically stable stationary point. For the considered parameters (30), the sector of linear stability of the linear part is

$$k > -0.05000004,$$

as follows from the Routh–Hurwitz criterion applied to $A + kBC^{\intercal}$. The derivative of the smoothed nonlinearity satisfies

$$0 < \varphi'_N(\sigma) \leq \Phi N = 40,$$

and therefore lies in this sector. Nevertheless, the system provides a counterexample to Kalman's conjecture, since a locally asymptotically stable stationary point coexists with stable periodic oscillations [Leonov et al., 2017; Mokaev, 2019; Kuznetsov, 2020].

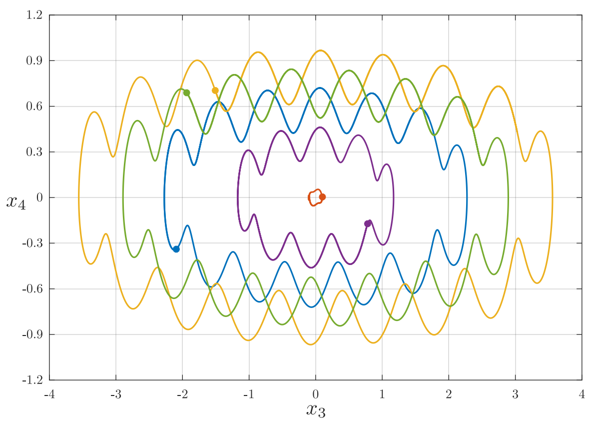

Figure 4. Periodic solutions of the Keldysh system with the original discontinuous characteristic with a quadratic term.

5 Conclusion

In this paper, the four-dimensional Keldysh system was studied as a nonlinear model of suppression of undesirable oscillations, written in the Lurie form with discontinuous nonlinear characteristics interpreted in the sense of Filippov. Two piecewise-linear approximations of the original Keldysh damper characteristic were considered. This made it possible to develop and apply the frequency-domain and LPRS-based analytical–numerical techniques, extending Boiko's approach to the four-dimensional system. For the relay and discontinuous piecewise-linear characteristics, the LPRS method, its analytical–numerical extension, numerical continuation, and direct simulations revealed symmetric and asymmetric periodic regimes, additional periodic solutions with more complicated switching structures. Continuation to the original discontinuous characteristic with a quadratic term revealed five periodic solutions, demonstrating multistability and the coexistence of self-excited and hidden oscillations in the Keldysh dynamics. The detected coexistence of stable equilibria and periodic solutions provides a motivation for further development of methods for estimating the boundary of global stability [Kuznetsov et al., 2020].

Acknowledgements

This work was supported by the Russian Science Foundation (grant No. 25-11-00147) and Saint Petersburg State University.

References

Akimova, E., Mokaev, R., Kuznetsov, N., and Boiko, I. (2021). On asymmetric periodic solutions in relay feedback systems. Journal of the Franklin Institute, 358 (1), pp. 363–380.

Boiko, I. (2008). Discontinuous Control Systems: Frequency-Domain Analysis and Design. Birkhäuser Boston.

Boiko, I., Kuznetsov, N., Mokaev, R., and Akimova, E. (2026). Frequency-domain analysis of a Keldysh-Like system. International Journal of Robust and Nonlinear Control, 36 (2), pp. 671–682.

Dolgopolik, M. and Fradkov, A. (2017). Nonsmooth and discontinuous speed-gradient algorithms. Nonlinear Analysis: Hybrid Systems, 25, pp. 99–113.

Dudkowski, D., Jafari, S., Kapitaniak, T., Kuznetsov, N., Leonov, G., and Prasad, A. (2016). Hidden attractors in dynamical systems. Physics Reports, 637, pp. 1–50.

Elsakov, A., Proskurnikov, A., and Smirnova, V. (2024). On cycle slipping in infinite-dimensional control systems with periodic nonlinearities. Cybernetics and Physics, 13 (4), pp. 281–287.

Filippov, A. (1988). Differential Equations with Discontinuous Righthand Sides. Kluwer, Dordrecht, The Netherlands. [Transl. from Russian: Moscow, USSR: Nauka, 1985].

Gelig, A., Leonov, G., and Yakubovich, V. (1978). Stability of Nonlinear Systems with Nonunique Equilibrium (in Russian). Nauka, Moscow, USSR. [English transl: Stability of Stationary Sets in Control Systems with Discontinuous Nonlinearities, 2004, World Scientific].

Keldysh, M. (1944). On dampers with a nonlinear characteristic. Tr. TsAGI (in Russian), 557, pp. 26–37.

Kiseleva, M. and Kuznetsov, N. (2015). Coincidence of Gelig-Leonov-Yakubovich, Filippov, and Aizerman-Pyatnitskii definitions. Vestnik St. Petersburg University. Mathematics, 48 (2), pp. 66–71.

Kolinichenko, A. (2024). The effect of diffusion on multistability and stochastic sensitivity in spatially extended systems. Cybernetics and Physics, 13 (2), pp. 123–129.

Kuznetsov, N. (2020). Theory of hidden oscillations and stability of control systems. Journal of Computer and Systems Sciences International, 59 (5), pp. 647–668.

Kuznetsov, N., Lobachev, M., Yuldashev, M., Yuldashev, R., Kudryashova, E., Kuznetsova, O., Rosenwasser, E., and Abramovich, S. (2020). The birth of the global stability theory and the theory of hidden oscillations. In 2020 European Control Conference Proceedings, pp. 769–774.

Leonov, G. and Kuznetsov, N. (2013). Hidden attractors in dynamical systems. From hidden oscillations in Hilbert-Kolmogorov, Aizerman, and Kalman problems to hidden chaotic attractors in Chua circuits. International Journal of Bifurcation and Chaos in Applied Sciences and Engineering, 23 (1). art. no. 1330002.

Leonov, G. and Kuznetsov, N. (2018a). On flutter suppression in the Keldysh model. Doklady Physics, 63 (9), pp. 366–370.

Leonov, G. and Kuznetsov, N. (2018b). On the Keldysh problem of flutter suppression. AIP Conference Proceedings, 1959 (1). art. num. 020002.

Leonov, G., Kuznetsov, N., Kiseleva, M., and Mokaev, R. (2017). Global problems for differential inclusions. Kalman and Vyshnegradskii problems and Chua circuits. Differential Equations, 53 (13), pp. 1671–1702.

Leonov, G. and Mokaev, R. (2017). Negative solution of the Kalman problem and proof of the existence of a hidden strange attractor via a discontinuous approximation method. Doklady Mathematics, 96 (1), pp. 415–418.

Leonov, G., Ponomarenko, D., and Smirnova, V. (1996). Frequency-Domain Methods for Nonlinear Analysis. Theory and Applications. World Scientific, Singapore.

Mokaev, R. (2019). Effective analytical-numerical methods for the study of regular and chaotic oscillations in dynamical systems. JYU Dissertations.

Utkin, V., Guldner, J., and Shi, J. (2017). Sliding Mode Control in Electro-Mechanical Systems. CRC Press.